Materials Science-Poland, *Vol. 27*, *No. 2*, *2009*

Controllable synthesis of ZnO nanostructures by a simple solution route

J. WANG[1,2*], S. HE[1], S. ZHANG[1], Z. LI[1], P. YANG[1], X. JING[1], M. ZHANG[1], Z. JIANG[2]

[1]College of Material Science and Chemical Engineering,
Harbin Engineering University, Harbin 150001, P R China

[2]College of Chemical Engineering, Harbin Institute of Technology, Harbin 150001, P.R. China

Flower-shaped ZnO nanostructures, composed of ZnO nanorods, and sphere-shaped ZnO nanoclusters, composed of ZnO nanosheets, were synthesized by reacting zinc acetate dehydrate with sodium hydroxide and polyethylene glycol-20000 (PEG-20000) at 180 °C for 4 h in solution. The thickness of individual nanosheets is about 40–60 nm. The nanorods are of hexagonal shape with sharp tips, and have basic diameters of ca. 450–550 nm. The ZnO nanostructures were characterized by scanning electron microscropy, transmission electron microscopy, X-ray diffraction, Fourier transform infrared, and Raman scattering measurements. The results demonstrated that the synthesized products are single crystalline with wurtzite hexagonal phase, the sphere-shaped ZnO grew in the [100] direction and the flower-shaped ZnO grew in the [001] direction.

Key words: *nanostructure; zinc oxide; optical properties; self-assembly*

1. Introduction

Controllable synthesis of semiconductors with nanostructures in terms of size and shape has been strongly motivated as their properties can be tailored by shape and size and novel applications can be investigated dependent on their structural properties [1–4]. Among various semiconductor nanostructures, a variety of ZnO nanostructures have been investigated, showing them to be one of the richest families of nanostructures [5]. ZnO is a key technological material that finds uses in a large number of applications in nanoelectronics, piezoelectric devices, optoelectronics, chemical sensors. ZnO has three key advantages. First, ZnO is a semiconductor with a direct wide band gap of 3.37 eV and a large exciton binding energy (60 eV). Second, because of its noncentral symmetry (wurtzite structure), ZnO is highly piezoelectric, which is a key property in building electromechanically coupled sensors and transducers. Finally, ZnO is a bio-safe and biocompatible material, and hence can be used for biomedical applications.

*Corresponding author, junwang@hrbeu.edu.cn

A variety of ZnO nanostructures have been reported in the literature, for instance, nanowires [6, 7], nanorods [8, 9], nanobelts [10], nanotubes [11], hexagonal nanocolumns [12], nanobows, nanorings, nanosprings [13, 14], nanostars [15], nanoflowers [16], microspheres and cages [17], aligned nanonails and nanopencils [18], nanosheet networks and hexagonal nanodisks [19]. In this study, we investigated a controllable synthesis of single-crystalline sphere-shaped ZnO and flower-shaped ZnO by a simple solution route.

2. Experimental

Zinc acetate dihydrate, sodium hydroxide and PEG-20000 were used as the source materials for the synthesis of ZnO, which was carried out at 180 °C in solution. All of the chemicals were purchased from the Tian Jin City Tian Xin Refined Chemical Corporation and used without further purification. Equivalent volumes of zinc acetate dihydrate (0.5 M) and sodium hydroxide (5 M) were mixed to obtain solution A. 1 g of PEG-20000 was dissolved in 4 ml of water by sonication to obtain solution B which was then added to 5 cm^3 of solution A to obtain solution C. 55 cm^3 of distilled water was added to solution C under stirring at room temperature to obtain solution D, Solution D was divided into two portions, and poured into Teflon tubes A and B, respectively. The Teflon tube A was immediately transferred to a Teflon-lined stainless steel autoclave, which was then heated at 180 °C for 4 h in an electric oven. The Teflon tube B was first kept at room temperature for 12 h, and then transferred to a Teflon-lined stainless steel autoclave, which was then heated at 180 °C for 4 h in an electric oven. ZnO crystalline powders were separated from the solution by filtration, washed with distilled water and dried. The ZnO samples obtained from tubes A and B were labelled A_1 and A_2, respectively.

General morphologies were identified using scanning electron microscopy (SEM). The SEM samples were made by dipping a copper grid into the suspension of ZnO powder in ethanol and dried at room temperature. The structure and crystal phases were determined by an X-ray powder diffractometry (XRD) with CuK_α radiation (λ = 1.54178 Å), with the Bragg angle ranging from 20° to 80°. The quality and composition of the synthesized sphere-shaped ZnO nanostructures were characterized by the Fourier transform infrared (FTIR) spectroscopy in the range of 400–4000 cm^{-1}. Optical properties were analyzed by the Raman scattering.

3. Results and discussion

3.1. Structural characterization of the sphere-shaped ZnO nanostructures

Figure 1 shows general scanning electron morphologies of synthesized samples. Figures 1a, b show the low magnification SEM images and Fig. 1c presents the high magnification images of the grown products of A_1. The images clearly show the flower-shaped structures that are composed of hexagonal nanorods. The magnified

image shows that flower-shaped structures are composed of hundreds of nanorods in the range of 450–550 nm with the length of 2–4 μm.

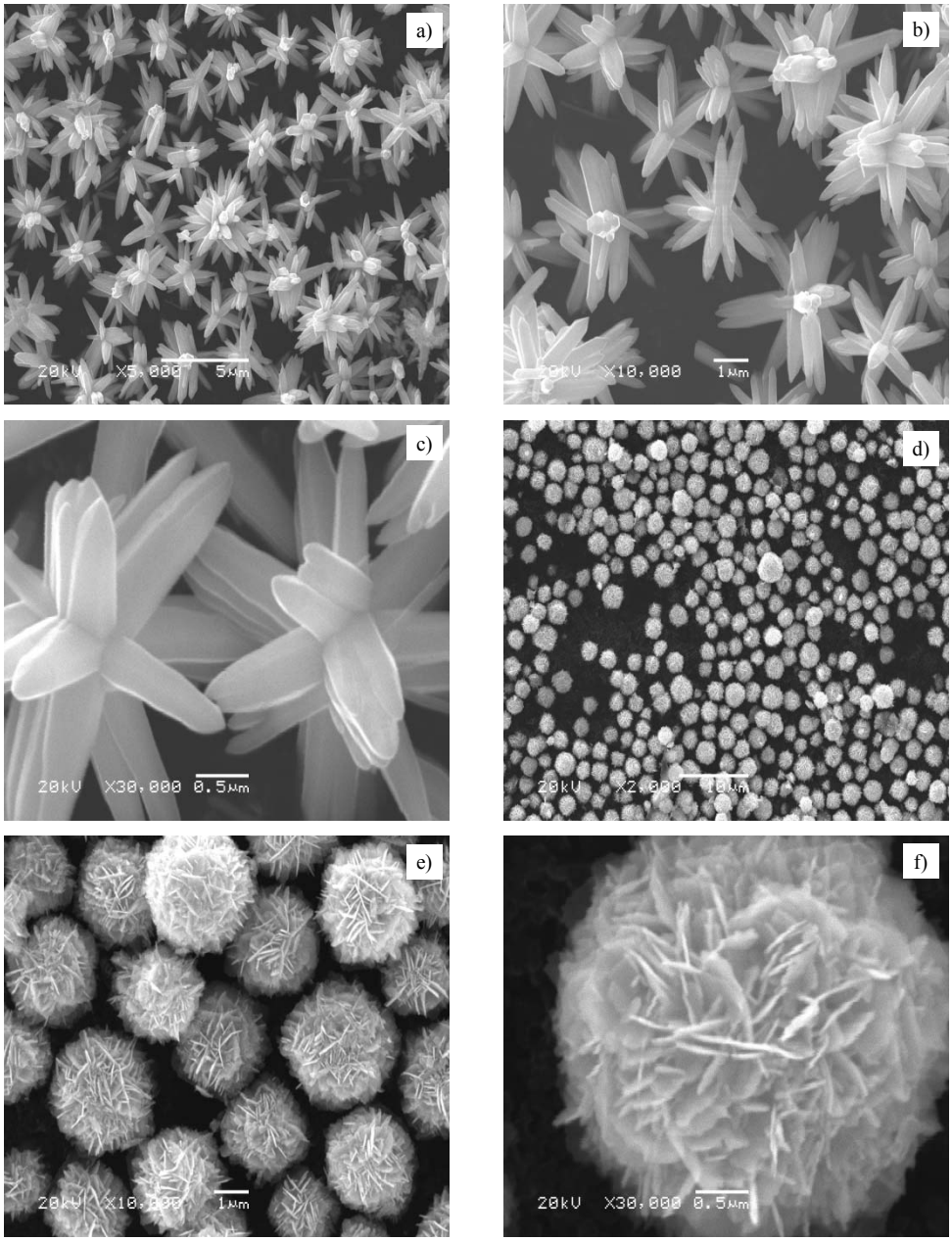

Fig. 1. SEM images of ZnO: a) overall product morphology of A_1, b) detailed views on average sized flowers of A_1, c) detailed view on an individual flower of A_1, d) overall product morphology of A_2, e) detailed views on average sized spheres of A_2, f) detailed view on an individual sphere of A_2

All the nanorods are seen to have originated from a single centre exhibiting flower-shaped morphologies. Figures 1d, e show low magnification SEM images, and Fig. 1f shows high magnification images of the grown products of A_2. The images clearly revealed that the sphere-shaped structures are formed by the accumulation of several hundred ZnO nanosheets. The size of each full array of a sphere-like structure is in the range of 3–4 μm.

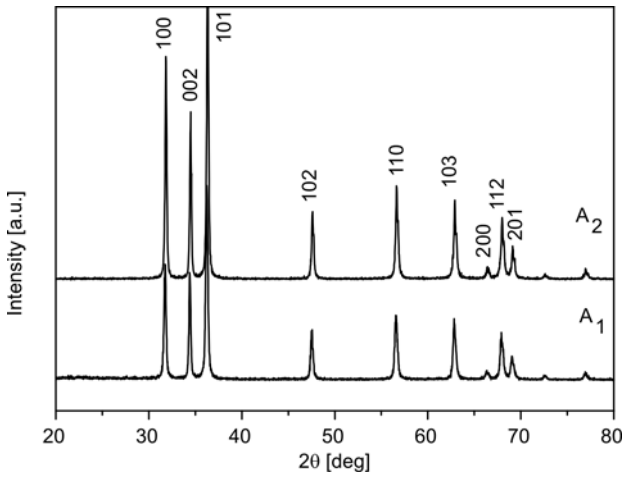

Fig. 2. Typical XRD pattern of the synthesized nanostructure: the indexed peaks correspond to the wurtzite hexagonal phase

Figure 2 presents the X-ray diffraction pattern of the synthesized powder. All of the indexed peaks are well matched with the bulk ZnO which confirmed that both A_1 and A_2 have wurtzite hexagonal structures. No other peaks related to impurities were detected in the spectra within the detection limit, which indicated that the synthesized powders are pure ZnO.

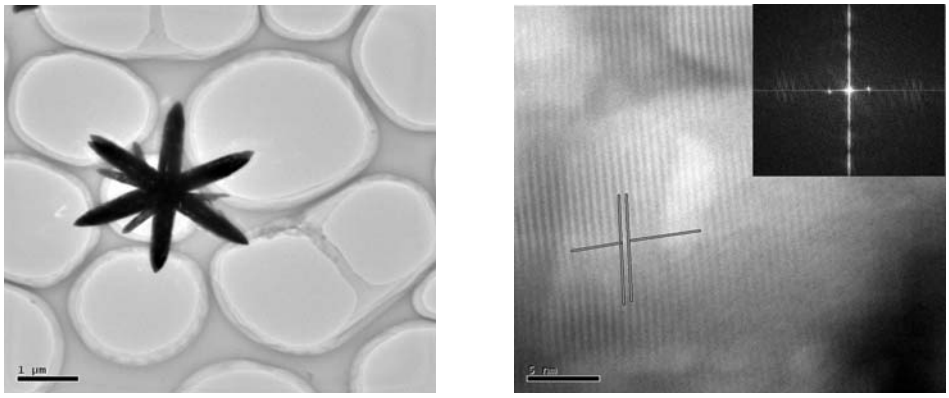

Fig. 3. Low magnification TEM image of the grown ZnO nanorods (a), HRTEM image showing the difference between two lattice fringes (b), being ca. 0.281 nm. The corresponding FT pattern (inset) is consistent with the HRTEM observation

Figure 3a shows a low magnification TEM image of the ZnO nanorods grown in the flower-shaped structures. The presence of ZnO nanorods is clearly evident from this image. The corresponding FFT pattern obtained from the shown nanorods confirmed that the synthesized products grew in the [001] direction. Figure 3b shows the HRTEM image of a nanorod. The lattice fringes between two adjacent planes is about 0.52 nm, being equal to the lattice constant of the ZnO, further indicating that the obtained structure is a wurtzite hexagonal phase and predominantly grown along the *c*-axis [001]. The corresponding FFT pattern (inset in Fig. 3b) is consistent with the HRTEM observation [20].

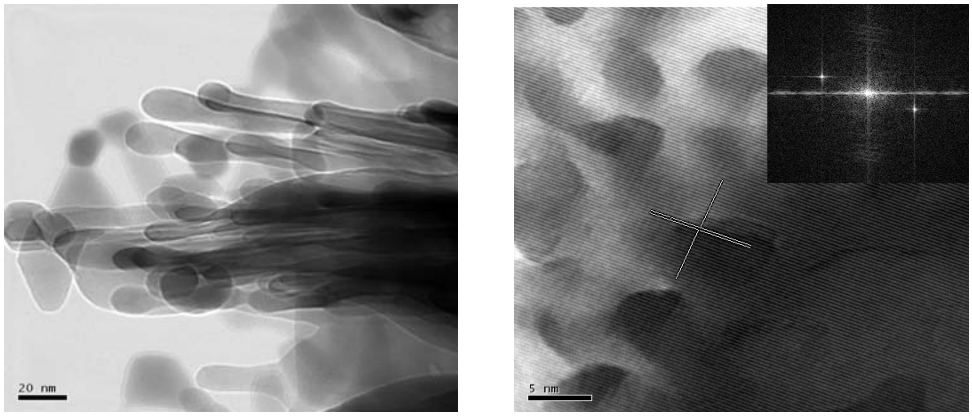

Fig. 4. Low magnification TEM image of the grown ZnO nanosheets (a) and HRTEM image showing the difference between two lattice fringes (b), which is about 0.281 nm. Corresponding FT pattern (inset) is consistent with the HRTEM observation

Figure 4a shows a low magnification TEM image of the ZnO nanosheets grown in the sphere-shaped structures. The ZnO nanosheets are clearly evident from this image. The corresponding FFT pattern obtained from the shown nanosheets confirmed that the synthesized products are single crystalline and grew in the [100] direction. Figure 4b shows a high resolution transmission electron microscopy (HRTEM) image of a nanosheet. The lattice fringe between two adjacent planes is about 0.28 nm, which is equal to the lattice constant of ZnO, indicating that the obtained structure has a wurtzite hexagonal phase and is predominantly grown in the *a* axis [100] direction. The corresponding FFT pattern (inset in Fig. 4b) is consistent with the HRTEM observation.

The composition and quality of the product was analyzed by the IR spectroscopy. Figure 5 (lower curve) shows the IR spectrum of A_1 in the range of 400–4000 cm^{-1}. The band at 571 cm^{-1} is correlated with zinc oxide [21]. The bands at 3200–3600 cm^{-1} correspond to the O–H vibration and the stretching vibration of C=O is observed at 1430 cm^{-1}. The IR spectrum of A_2 in the range of 400–4000 cm^{-1} is also shown in Fig. 5 (upper curve). The band at 560 cm^{-1} is correlated with zinc oxide. The bands at 3200–3600 cm^{-1} correspond to the O–H vibration and the stretching vibration of C=O is observed at 1437 cm^{-1}.

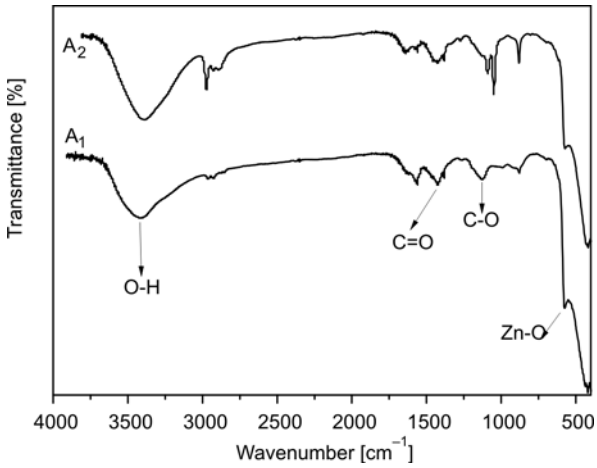

Fig. 5. Typical IR spectra of the synthesized nanostructures

3.2. Optical properties of the sphere-shaped ZnO nanostructures

The optical properties of the synthesized sphere-shaped ZnO nanostructure were investigated by Raman scattering. The Raman spectra are sensitive to the crystal quality, structural defects and disorders of the grown products. With the wurtzite hexagonal structure, ZnO belongs to the C_{6V}^4 with two formula units per a primitive cell. The primitive cell includes two formula units in which all the atoms occupy the 2b sites of

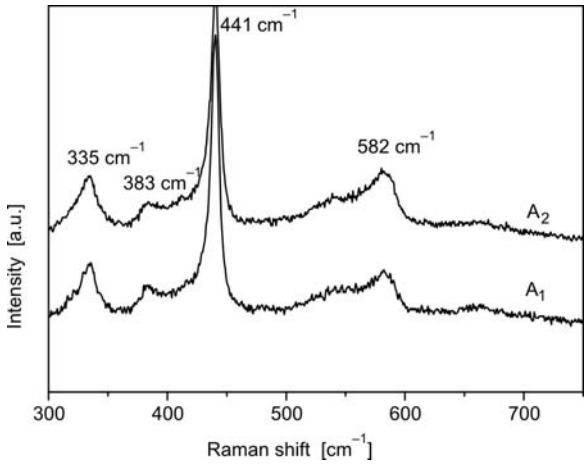

Fig. 6. Typical Raman spectra of the synthesized nanostructures

the C_{3V} symmetry. The group theory predicts, the existence of the following optical modes at the Γ point of the Brillouin zone: $\Gamma = A_1 + 2B_1 + E_1 + 2E_2$. The A_1, E_1 and E_2 modes are Raman active. Furthermore, the A_1 and E_1 are infrared active and split into

longitudinal optical (OP) components and transverse optical (TO) components [22]. Figure 6 shows the Raman spectrum of the synthesized powder. A sharp and strong peak observed at 441 cm^{-1} is attributed to the optical phonon E_2 mode of the ZnO and a characteristic Raman active peak for the wurtzite hexagonal phase of ZnO [23]. Two very small peaks at 335 and 383 cm^{-1} observed in the spectrum are assigned as E_{2H}–E_{2L} (multiphonon process) and A_{1T} modes, respectively. Additionally, a very suppressed peak at 582 cm^{-1} the spectrum was assigned as E_{1L} mode [24, 25]. The origin of the E_{1L} mode in the Raman scattering is explained by the impurities and structural defects (oxygen vacancies and Zn interstitials) of the synthesized products. The presence of the high intensity E_2 mode with the suppressed and very weak E_{1L} peak in the Raman scattering indicated that the synthesized sphere-shaped ZnO nanostructures have good crystal quality and possess the wurtzite hexagonal crystal structure.

4. Conclusion

Synthesis of sphere-shaped ZnO nanostructures composed of ZnO nanosheets and synthesis of flower-shaped ZnO nanostructures composed of ZnO nanorods were successfully achieved by reacting zinc acetate dihydrate, sodium hydroxide and PEG-20000 at 180 °C for 4 h in solution. Detailed structural characterizations demonstrated that the synthesized products are single crystalline with the wurtzite hexagonal phase, the obvious differences are clearly evident from the SEM and TEM data.

Acknowledgement

We gratefully acknowledge the financial support of this research by the Key Technology R&D program of Heilongjiang Province (No. TB06A05), basic research fund of Harbin Engineering University (No. mzj07076) and Science Fund for Young Scholar of Harbin City (No. 2008RFQXG028).

References

[1] ALIVISATOS A.P., Science, 271 (1996), 933.
[2] BEEK W.J.E., WIENK M.M., JANSSEN R.A.J., Adv. Mater., 16 (2004), 1009.
[3] BEEK W.J.E., WIENK M.M., EMERINK M.K., YANG X., JANSSEN R.A.J., J. Phys. Chem. B, 109 (2005), 9505.
[4] XIA Y., YANG P., SUN Y., WU Y., MARE B., GATES B., YIN Y., KIM F., YAN H., Adv. Mater., 15 (2003), 323.
[5] WANG Z.L., Mater. Today, 7 (2004), 26.
[6] SEKAR A., KIM S.H., UMAR A., HAHN Y.B., J. Cryst. Growth, 277 (2005), 471.
[7] UMAR A., RA H.W., JEONG J.P., SUH E.K., HAHN Y.B., Korean J. Chem. Eng., 23 (2006), 499.
[8] UMAR A., KIM S.H., LEE Y.S., NAHM K.S., HAHN Y.B., J. Cryst. Growth, 282 (2005), 131.
[9] UMAR A., KARUNAGARAN B., SUH E.K., HAHN Y.B., Nanotechn., 17 (2006), 4072.
[10] HUGHES W.L., WANG Z.L., Appl. Phys. Lett., 82 (2003), 2886.
[11] ZHANG B.P., BINH N.T., WAKATSUKI K., SEGAWA Y., YAMADA Y., USAMI N., KOINUMA H., Appl. Phys. Lett., 84 (2004), 4098.
[12] UMAR A., HAHN Y.B., Appl. Phys. Lett., 88 (2006), 17312.

[13] HUGHES W.L., WANG Z.L., J. Am. Chem. Soc., 126 (2004), 6703.
[14] GAO P.X., WANG Z.L., J. Appl. Phys., 97 (2005), 44304.
[15] UMAR A., LEE S., LEE Y.S., NAHM K.S., HAHN Y.B., J. Crystal Growth., 277 (2005), 479.
[16] UMAR A., LEE S., IM Y.H., HAHN Y.B., Nanotechn., 16 (2005), 2462.
[17] UMAR A., KIM S.H., IM Y.H., HAHN Y.B., Superlatt. Microstruct., 39 (2006), 238.
[18] SHEN G., BANDO Y., IU B., GOLBERG D., LEE C.J., Adv. Func. Mater., 16 (2006), 410.
[19] UMAR A., HAHN Y.B., Nanotechn., 17 (2006), 2174.
[20] WAHAB R., ANSARI S.G., KIM Y.S., SEO H.K., KIM G.S., KHANG G., SHIN H.-S., Mater. Res. Bull., 42 (2007), 1640.
[21] LILI W., YOUSHI W., YUANCHANG S., HUIYING W., Rare Metals, 25 (2006), 68.
[22] DAMEN T.C., PORTO S.P.S., TELL B., Phys. Rev., 142 (1966), 142.
[23] XING Y.J., XI Z.H., XUE Z.Q., ZHANG X.D., SONG J.H., WANG R.M., XU J., SONG Y., ZHANG S.L., YU D.P., Appl. Phys. Lett., 83 (2003), 1689.
[24] RAJALAKSHMI M., ARORA A.K., BENDRE B.S., MAHAMUNI S., J. Appl. Phys., 87 (2000), 2445.
[25] VANHEUSDEN K., SEAGER C.H., WARREN W.L., TALLANT D.R., VOIGT J.A., J. Appl. Phys., 79 (1996), 7983.

Received 11 August 2008
Revised 9 January 2009